



**HAL**  
open science

# The ornamentation steps of the Bull Rotunda of the Lascaux cave give new insights into the Upper Palaeolithic natural life cycle

Ina Reiche, Colette Vignaud, Emilie Chalmin, Michel Menu, Jean-Michel Geneste

## ► To cite this version:

Ina Reiche, Colette Vignaud, Emilie Chalmin, Michel Menu, Jean-Michel Geneste. The ornamentation steps of the Bull Rotunda of the Lascaux cave give new insights into the Upper Palaeolithic natural life cycle. *Archaeometry*, In press, 10.1111/arcm.12960 . hal-04498458

**HAL Id: hal-04498458**

**<https://hal.science/hal-04498458v1>**

Submitted on 11 Mar 2024

**HAL** is a multi-disciplinary open access archive for the deposit and dissemination of scientific research documents, whether they are published or not. The documents may come from teaching and research institutions in France or abroad, or from public or private research centers.

L'archive ouverte pluridisciplinaire **HAL**, est destinée au dépôt et à la diffusion de documents scientifiques de niveau recherche, publiés ou non, émanant des établissements d'enseignement et de recherche français ou étrangers, des laboratoires publics ou privés.

**The ornamentation steps of the Bull Rotunda of the Lascaux cave give new insights into the Upper Palaeolithic natural life cycle**

Journal:	<i>Archaeometry</i>
Manuscript ID	ARCH-09-0737.R1
Wiley - Manuscript type:	Original Article
Date Submitted by the Author:	n/a
Complete List of Authors:	Reiche, Ina; Chimie ParisTech, Institut de Recherche de Chimie-Paris (IRCP); CNRS, FR 3506 CNRS - Centre de recherche et de restauration des musées de France Vignaud, Colette; Centre de Recherche et de Restauration des Musées de France, Chalmin, Emilie; Université Savoie Mont-Blanc, EDYTEM Menu, Michel; Centre de Recherche et de Restauration des musées de France; The Cyprus Institute, APAC Labs Geneste, Jean-Michel; PACEA
Keywords:	Lascaux cave, creation steps, manganese and iron oxides, SEM-EDX, TEM-EDX-SAED, Palaeolithic paintings, natural life cycle
Abstract:	Although the ornamentation of the Lascaux cave seems relatively homogeneous in style, the analysis by scanning and transmission electron microscopy of 32 micro-samples from the figures of the Hall of the Bulls (Bull Rotunda) and one desquamated sample from the soil highlighted different paint pots. The black and red paint matters with their associated mineralogical phases were extensively characterized. Considering previous stylistic and superimposition studies, we were eventually able to confirm five creation steps of monothematic figures ("assemblages") based on the chemical and mineralogical characteristics. Further interpretations in terms of the rhythm and temporal framework of the Hall of the Bulls (Bull Rotunda) of the Lascaux cave could be reinforced. Some particular representations such as the black cave bear and one of the cross shaped signs were shown to be likely added at later moments by different hands because their paint pots were different from those of the Bull Rotunda and similar to that of other representations in deeper rooms of the Lascaux cave. We also found that the paint matter of the Bull Rotunda was different than those of other Palaeolithic cave sites on a more regional scale indicating a very local sourcing.
Note: The following files were submitted by the author for peer review, but cannot be converted to PDF. You must view these files (e.g. movies) online.	
Figure7_R.svg	

1  
2  
3  
4  
5  
6  
7  
8  
9  
10  
11  
12  
13  
14  
15  
16  
17  
18  
19  
20  
21  
22  
23  
24  
25  
26  
27  
28  
29  
30  
31  
32  
33  
34  
35  
36  
37  
38  
39  
40  
41  
42  
43  
44  
45  
46  
47  
48  
49  
50  
51  
52  
53  
54  
55  
56  
57  
58  
59  
60



## The ornamentation steps of the Bull Rotunda of the Lascaux cave give new insights into the Upper Palaeolithic natural life cycle

Ina Reiche<sup>1,2\*</sup>, Colette Vignaud<sup>3</sup>, Emilie Chalmin<sup>4</sup>, Michel Menu<sup>5</sup>, Jean-Michel Geneste<sup>6</sup>

1 Fédération de recherche New AGLAE, FR3506 CNRS/Ministère de la Culture, Palais du Louvre, Paris, France.

2 PSL Université, Chimie Paristech, Institut de recherche de Chimie Paris, UMR 8247 CNRS, PCMTH, Paris, France

3 former address: Laboratoire du Centre de recherche et de restauration des musées de France, C2RMF-UMR171 CNRS, Palais du Louvre, Paris, France, present address: Colette.vignaud@noos.fr

4 EDYTEM, UMR CNRS 5204, Université Savoie Mont-Blanc, Le Bourget-du-Lac, France

5 former address: Centre de recherche et de restauration des musées de France, C2RMF, Palais du Louvre, Paris, France, present address: APAC Labs, The Cyprus Institute, Nicosia, Cyprus

6 PACEA UMR 5199 CNRS/Ministère de la culture & Université de Bordeaux, Bordeaux, France

\* corresponding author: ina.reiche@chimieparistech.psl.eu

### Abstract

Although the ornamentation of the Lascaux cave seems relatively homogeneous in style, the analysis by scanning and transmission electron microscopy of 32 micro-samples from the figures of the *Hall of the Bulls (Bull Rotunda)* and one desquamated sample from the soil highlighted different paint pots. The black and red paint matters with their associated mineralogical phases were extensively characterized. Considering previous stylistic and superimposition studies, we were eventually able to confirm five creation steps of monothematic figures ("assemblages") based on the chemical and mineralogical characteristics. Further interpretations in terms of the rhythm and temporal framework of the *Hall of the Bulls (Bull Rotunda)* of the Lascaux cave could be reinforced. Some particular representations such as the black cave bear and one of the cross shaped signs were shown to be likely added at later moments by different hands because their paint pots were different from those of the Bull Rotunda and similar to that of other representations in deeper rooms of the Lascaux cave. We also found that the paint matter of the Bull Rotunda was different than those of other Palaeolithic cave sites on a more regional scale indicating a very local sourcing.

### Introduction. Previous work on the Lascaux cave and paint samples

Electron microscopy can bring to light invisible information about rock art. The Lascaux cave is one of the most famous decorated caves in the world dating back to the Magdalenian period. Its rock art has been studied in detail by N. Aujoulat (Aujoulat, 2004). Lascaux's paintings and graphical entities seem to have been created in relatively short period of time in all parts of the cave (Leroi-Gourhan and Allain, 1979), likely a few centuries at the height of the temperate interstadial of Lascaux. There are many instances

1  
2  
3 of enrichments, repainting and retouching of the parietal decorations, but there is an  
4 obvious unity of style in Lascaux. Recent radiocarbon dates of five reindeer scraps from  
5 the main sectors of the cave (*Axial gallery, Passage, Nef, Puits*) place the occupation of  
6 the cave around 17,600 uncal. BP (meaning 21,500-21,000 cal. BP) (Ducasse and  
7 Langlais, 2019) but there is still no date of paintings.  
8

9  
10 The results obtained from the physicochemical analysis of 17 micro-samples (GLAS26,  
11 GLAS45-46, GLAS50-55, GLAS62, GLAS101-107) of isolated scenes at different  
12 locations of the Lascaux cave have already been reported elsewhere following a strategy  
13 of panels or coherent scenes such as the *scène du Puits* (Aujoulat et al., 2002), *blasons*  
14 (Chalmin et al., 2004) and the *bisons adossés* (Vignaud et al., 2006) as well as two  
15 isolated figures, horse and deer (Chalmin, 2003). The different scenes were related in  
16 stylistic accordance, method of application and paint matter. It was brought to light that  
17 paint matter was deliberately prepared as a function of a specific use. As an example,  
18 Lascaux' artists used different paint matters for the *blasons'* rectangles, each with a  
19 singular shade (Chalmin et al., 2004). Beyond these preparation specific features, it turned  
20 out that there was a large palette of manganese (Mn) oxide minerals and various qualities  
21 of haematite that allowed painters to obtain subtle colour hues (Aujoulat et al., 2002;  
22 Chalmin et al., 2004; Vignaud et al., 2006). Haematite is less discriminative than the black  
23 Mn oxide based phases in distinguishing prehistoric figures. Scanning Electron  
24 Microscopy (SEM) observations on microscale only allow the identification of Mn oxide  
25 agglomerates. For the discrimination of different mineralogical phases, Transmission  
26 Electron Microscopy (TEM) coupled with an Energy Dispersive Analysing system (EDS)  
27 and Selected Area Electron Diffraction (SAED) is required. These new criteria allow new  
28 insights into the different paint recipes of the prehistoric artists of Lascaux.  
29  
30

31  
32 Despite the homogeneity of the style in Lascaux, previous results indicated that different  
33 paint matters and preparations allow the identification of groupings ("assemblages") that  
34 contribute to a better understanding of the various execution sequences of  
35 representations. Furthermore, technological information on raw materials, preparation,  
36 applications and also possibly economic activities (choice of raw materials, diversity,  
37 specific selection) can be obtained.  
38

39  
40 The *Bull Rotunda* is an enigmatic chamber and its decoration seems to be among the first  
41 one to be executed in the Lascaux cave. It is 18 m long, 7 m large and 4-5 m high with a  
42 surface of 117 m<sup>2</sup> (Aujoulat, 2004) (Fig. 1.) The quality of the wall is not suitable for  
43 engraving but favourable for painting because of a homogeneous very indurated white  
44 carbonate concretion with relatively large grains (from 5 to 20 mm in diameter) and high  
45 reflective power that covers the entire substrate rock in the *Rotunda*. There is a change in  
46 the colour of the substrate that materializes a baseline used as an imaginary soil for most  
47 of the figures in the room. Only a few gaps in the carbonate concretion, scale imprints and  
48 corroded beaches disturb the homogeneity of this covering and there is the presence of  
49 macro-cupules in the lower part of the panel. Among the animals, the *horses* are the most  
50 numerous (N=17) then *aurochs* (bulls) and *cows* (N=11) and finally *deer* (N=5). There is  
51 also a single *bison* (N=1), a *unicorn* (N=1) and a *cave bear* (N=1) (35) (Fig. 2 and 3  
52 (Aujoulat, 2004)). The animal representation of the *unicorn* (mysterious animal actually  
53 represented with two horns) is unique by the way. There are also other representations of  
54 rare animal species such as a *cave bear*. The *bear* is superimposed on the initially  
55  
56  
57  
58  
59  
60

1  
2  
3 executed large ventral line of the first bull on the right side in the *Rotunda* (Fig. 3, 1D101).  
4 It was discovered thanks to its muzzle and its ears, which went over the ventral line of the  
5 *black bull*.  
6

7 Animals are either monochrome (black or red) or bichrome with different colour  
8 associations (black and red, brown or yellow). Some figures present different colour  
9 gradients such as the *brown horse* 1G204 with colours ranging from light brown to black  
10 and the *deer* 1G214 with colours from yellow to black. Basically, large *black bulls* and *red*  
11 *cows* are found in the *Rotunda*: 3.5 m (L) X 3.0 m (H) for bull 1G203 (Fig. 2), 4.6 m (L) X  
12 2.8 m (H) for bull 1G205 (Fig. 2) and 5.6 m (L) X ca. 3 mm (H) for bull 1D101 (Fig. 3). They  
13 are the largest representations found in all European Palaeolithic art. However, the size  
14 contrasts strongly between certain species of animals. *Horses* are bichrome and smaller  
15 in size (Aujoulat, 2004).  
16  
17

18 Different methods of paint application were identified: painting with a brush, a stamp,  
19 spraying and/or stencil drawing. While their study and interpretation are not in the focus  
20 of the present work, we may mention, as an example, the black dorsal lines of the *bulls*  
21 were executed using a series of very close punctuations avoiding any pointillism effect.  
22 The regularity of point diameters indicates a similar or even the same tool was used. A  
23 consistent application technique was also used for the *red cow* representations. In the  
24 lower part of the figures, spraying was used, whereas in the upper part of the figures, paint  
25 was applied with a brush, due to the (in)accessibility of the wall. More details are reported  
26 elsewhere (Aujoulat, 2004).  
27  
28

29 A. Laming-Empeire suggested in 1959 that the identification of groups in different parts  
30 of the cave ("assemblages") corresponded to a conscious order in the distribution of  
31 animals, as well as a combination of size, species and direction of animals (Laming-  
32 Empeire, 1959). N. Aujoulat also set the sequence of execution steps in the *Bull*  
33 *Rotunda* in the 1980-90's, each composed of different monothematic animal  
34 representations. According to stylistic and macro-photographical observations of the  
35 walls, he proposed five steps (Aujoulat, 2004): step 1 corresponded to a series of  
36 monochromatic *horses*, step 2 to a series of *bichrome and polychrome horses* including  
37 the *unicorn*, step 3 to a series of *black bulls*, step 4 to a series of *red cows* and step 5  
38 finally to a series of *deer* (step 5). J.-M. Geneste further interpreted this sequence in 2021  
39 on the basis of stylistic and superimposition studies in terms of the natural life cycle of the  
40 Upper Palaeolithic hunter societies, and proposed the different steps of monothematic  
41 animal depictions to be related to the natural rhythm of the animal herds in the prehistoric  
42 landscape, e.g. seasons (Geneste, 2021).  
43  
44  
45

### 46 **Aim of this work**

47 In the present work we discuss the consistency of the hypothesized execution steps in  
48 terms of different paint pots, especially the colouring phases, used for the different animal  
49 series in the *Bull Rotunda*. Electron microscopic analyses and observations of micro-  
50 samples taken from different paintings in the emblematic *Bull Rotunda* of the Lascaux  
51 cave allow the characterisation of these paint pots. We can infer from different paint pots  
52 different execution steps under the following conditions: first, different paint matters can  
53 be identified in the executed prehistoric graphical entities; second, the paint matter is  
54 characteristic at the scale of the micro-samples for each figure, and can thus be  
55  
56  
57  
58  
59  
60

1  
2  
3 considered representative enough of the figures on the wall; and third, it can be postulated  
4 that one single hand or a very small group of artists created in the cave a series of  
5 stylistically similar figures, and completed them in a short period of time (nearly  
6 simultaneously), when the same or a similar type of components is found in the micro-  
7 samples corresponding to a particular series of prehistoric figures.  
8

9  
10 Based on this, it was assumed that series of figures could be defined according to their  
11 chemical and mineralogical characteristics as observed by electron microscopy.  
12 Additionally, we suggested that it was possible to attribute, from a stylistically, chemically  
13 and mineralogically homogeneous group of prehistoric figures of the same colour, to a  
14 consistent step of execution. However, it is not possible to determine the duration or the  
15 number of artists involved in a particular execution step (although sometimes individual  
16 hands of prehistoric artists could be stylistically identified (Fritz and Tosello, 2015)) nor the  
17 time lapse between different execution steps.  
18

19 By identifying different steps of execution in the *Bull Rotunda* we intended to reinforce the  
20 interpretation of the ornamentation steps as related to the temporal natural life cycle of the  
21 Upper Palaeolithic hunter-gatherer society, e.g. seasons.  
22

### 23 **Studied material and methods**

24  
25 This study summarized the results of the analyses of 33 micro-samples taken from  
26 different figures in the *Bull Rotunda* of the Lascaux cave, including the desquamated  
27 sample collected from the soil. Three field trips were authorized to take micro-samples: 25  
28 micro-samples were taken in 1996 (GLAS1-25), 3 in 1999 (GLAS61-63) and 4 in 2005  
29 (GLAS117-120) as well as one desquamated sample from the soil (LAS121). The two field  
30 trips in 1996 and 1999 took place before the closing of the cave, while the one in 2005  
31 occurred after. Micro-samples of black, red and yellow graphical entities were taken using  
32 a sterilized scalpel. On the left wall, we counted 21 samples from ten animal figures  
33 (sample GLAS 1-2: *black unicorn* 1G201, GLAS3-6: *bichrome horse* G202, GLAS7-8:  
34 *bichrome horns of the bull* 1G203, GLAS10: *brown horse* 1G204, GLAS11: *red deer*  
35 *1G212*, GLAS12-13: *bichrome deer* 1G214 and a *black horse*, numbered here 1G206bis,  
36 GLAS15: *red cow* 1G206, GLAS16: *small black horse*, GLAS17-18: *black bull* 1G205) and  
37 two signs (GLAS9: 1G223 (could also correspond to the muzzle of a hidden animal) and  
38 GLAS 14:1G226). On the right, twelve samples from five animal figures (GLAS 22-23,  
39 118: *black bull* 1D101 , GLAS20: *black bull* 1D102 , GLAS24: *red cow* 1D103, GLAS26:  
40 *red calf* 1D108, GLAS25,117: *black bear* 1D107 and two *signs* (GLAS 19: *cross* 1D112,  
41 GLAS21: 1D114) were studied, as well as a desquamated sample (LAS121) laying on the  
42 floor (Fig. 1, Table 1) and GLAS119 corresponding to the red spot on the bench seat.  
43  
44  
45

46 We used optical microscopy (OM), SEM-EDS, TEM-EDS and TEM-SAED to characterize  
47 the large set of paint micro-samples on the micro- and the nanoscale. The sample LAS121  
48 was prepared as a cross-section inserted in polyester resin and then polished. The other  
49 samples were studied without resin inclusion by OM and SEM. Only when the paint matter  
50 was concentrated enough in the micro-sample was a sample prepared for TEM  
51 observations, which requires invasive preparation.  
52  
53

### 54 Optical microscopy

55  
56  
57  
58  
59  
60



1  
2  
3 The paint cross-section and the micro-samples were examined under a light microscope  
4 (NIKON Eclipse LV 100ND) and photographed without any preparation.  
5

### 6 SEM-EDS

7  
8 The micro-samplings were deposited without any preliminary preparation directly into a  
9 metallic cup to avoid charge phenomena, nickel was chosen in order to avoid interfering  
10 with detected elements in the EDS spectrum .  
11

12 The cross-section is carbon-coated to enable charge evacuation.

13  
14 For this study, a Jeol JSM-840 SEM and a Philips XL 30 CP SEM were used, both  
15 equipped with an EDX Link Isis 300 analysis system. An acceleration voltage of 20 kV of  
16 the electrons with a beam current of about 100  $\mu$ A was generally used.  
17

### 18 TEM- EDS and TEM-SAED

19  
20 Each selected sample was ground in an agate mortar. The obtained powder was  
21 dispersed ultrasonically in ethanol and then a drop of this preparation was deposited on a  
22 carbon-coated copper (Cu) or gold (Au) grid. The TEM observations were carried out at  
23 200 kV on the sample grid using a JEOL 2000FX microscope equipped with a Link Isis  
24 EDS. Using a double tilted object holder, electron diffraction (SAED) is carried out and the  
25 crystallographic structure of the poly-crystals was then recorded. If individual crystals were  
26 large enough, a single-crystal diffraction pattern could be recorded on each one. Knowing  
27 its chemical composition, the single-crystal identity and its zone axis is identified using the  
28 Carine software®.  
29

## 30 **Results**

### 31 **Microscale morphological and chemical characteristics**

32  
33  
34 Optical microscope observations of the micro-samples enabled us to evaluate the  
35 thickness, the colour and the texture of the pigment. We were also able to extract the paint  
36 matter from the wall support. The thickness of the micro-samples was approx. between  
37 50 and 500  $\mu$ m. This thickness allowed good access to the distribution of each component  
38 in the paint matter and avoided disturbance from potential components coming from the  
39 limestone support or various posterior encrusts (Fig. 4a-d).  
40

41  
42 The cross section LAS121 corresponded to a red paint sandwiched between a thin outer  
43 layer of transparent calcium carbonate and a thick layer of calcium (Ca) carbonate from  
44 the wall support. The paint sample was actually a peeling off of the wall well below the  
45 paint. The paint layer in the cross section contained a thin layer of about 5 to 10  $\mu$ m of  
46 inhomogeneous clay rich in iron. Punctually, iron (Fe) oxides were visible in the form of  
47 platelets of 1 to 2  $\mu$ m in the electron micrograph (Fig. 4b and 5a).  
48

49  
50 SEM observations of the micro-samples showed micro-morphological characteristics in  
51 addition to chemical analysis (EDS) (Table 1). All black samples were agglomerates  
52 composed of different types of manganese (Mn) oxides, some containing additionally  
53 aluminosilicates material. Chemically, three types of Mn oxides are found: pure Mn oxide,  
54 Barium (Ba)-containing Mn oxide and Mn oxide with variable amounts of Ba and  
55 potassium (K). Different morphologies can be identified, but not different crystallographic  
56 structures. For example, the *cave bear* sample GLAS117 showed three morphologies of  
57  
58  
59  
60



1  
2  
3 Mn oxides: simple Mn oxide or hydroxide (fig. 5c) and at higher magnification fines needles  
4 of a Ba-bearing Mn oxide as well as cubic Ca carbonate (Fig 5d).  
5

6 Aluminosilicates were present in most of the black paints; quartz was more rare. The  
7 presence of a phase combining calcium (Ca) and phosphorus (P) could be noticed in only  
8 two samples (black punctuations GLAS21 and *cave bear* GLAS25). In black signs mercury  
9 (Hg) was also as small droplets. This was likely contemporary pollution, as the  
10 temperature of the cave was controlled using Hg-thermometers, that were frequently  
11 broken inside the cave. Morphologically, platelet-like crystals, sheets, sticks, needle-  
12 shaped, filaments, balls and spherical grains as well as “desert roses” and meshes could  
13 be described in these Mn oxide blocs (Table 1). The morphology corresponding to the  
14 crystallization modus did not, however, give any information about the types of  
15 crystallographic phase present in the Mn oxides.  
16  
17

18 Red paints were composed of iron (Fe) oxides of different crystal shapes. Fibrous crystals  
19 are found as well as needles, platelet-like crystals and spherical grains. Chemically, other  
20 natural phases such as quartz, aluminosilicates and calcium carbonate were observed  
21 besides Fe oxide. Particularly, one Ca and P-based phase (probably hydroxyapatite) was  
22 also identified in most samples. Further minor elements like K and titanium (Ti) were  
23 detected but cannot be attributed to a specific compound.  
24

25 The yellow paint sample was composed of a mixture of iron oxide, a high amount of  
26 calcium carbonate possibly from the wall support or from recrystallization process, some  
27 aluminosilicates and a Ca-P based compound, likely hydroxyapatite.  
28

29 Brown paints were composed of mixtures of Fe and Mn oxides in addition to  
30 aluminosilicates, calcium carbonate, quartz and calcium sulphate (likely gypsum). The  
31 latter phase possibly originated from weathering processes. Interestingly, the presence of  
32 a Ca and P-based phase was observed for the red flat paints (filling). Manganese oxide  
33 crystal agglomerates were needle- or fibre-shaped and Fe oxides were sheet-like.  
34  
35

36 Further discrimination of the crystallographic structures present in the paint samples is not  
37 possible. Therefore, nanoscale observations using TEM-EDS and TEM-SAED were  
38 required.  
39

### 40 **Nanoscale morphological and crystallographic characteristics**

41 TEM observations allowed the determination of the nano-morphological characteristics at  
42 the scale of individual crystals. Chemical analysis by EDS on individual crystals allows  
43 identifying characteristic minor elements associated to a special crystal in the phase  
44 mixtures. After chemical identification of the individual crystal, crystallographic phase and  
45 crystal orientation (zone axis) identification was performed on the individual crystal  
46 electron diffraction patterns (SAED).  
47  
48

49 All black samples were either identified as cryptomelane (simple non-stoichiometric Mn  
50 oxide:  $[(Ba,K)Mn_8O_{16}].xH_2O$ ) alone or mixtures of cryptomelane with hollandite  
51  $(BaMn_8O_{16}.xH_2O)$  or todorokite  $([(Ba,Ca,K,Na)Mn_6O_{12}].H_2O)$  (Fig.6 a-c). These  
52 crystallographic phases correspond to Mn oxides with variable amounts of Ba and K,  
53 which is consistent with the SEM-EDS observations. From a morphological point of view,  
54 there were generally longitudinal single-crystals, and special meshes were found for the  
55  
56  
57  
58  
59  
60

1  
2  
3 todorokite phase. The presence of K could directly be linked to the Mn oxide phase  
4 cryptomelane and not to the aluminosilicates as it was identified on individual crystals. In  
5 some cases, the K-bearing Mn oxide was prevalent with respect to the Ba-containing Mn  
6 oxide (Table 1).  
7

8 Particular phases were observed in the *cave bear* (1D107) paint samples (GLAS25 and  
9 GLAS117) that showed a mixture of pyrolusite ( $\text{MnO}_2$ ), manganite ( $\text{MnOOH}$ ) and  
10 romanechite ( $\text{Ba}_2\text{Mn}_5\text{O}_{10}\cdot x\text{H}_2\text{O}$ ) (Fig. 7a-c) and the black sample GLAS19 corresponding  
11 to the *cross-shaped sign* 1D112, which was composed of a mixture of cryptomelane and  
12 magnetite ( $\text{Fe}_3\text{O}_4$ ) (Fig. 7d).  
13

14 TEM-SAED provided evidence of haematite crystals in every red paint sample. Most of  
15 the haematite was poorly crystallized without characteristic shape and was mixed within  
16 aluminosilicates, but two types of lamellar crystals (lamellar sheets with hexagonal shape  
17 (type I) and lamellar sheets of trapezoidal shape (type II)), could be found and were  
18 chosen for electron diffraction. Both crystal types showed more or less regular features  
19 and variable dimensions. Hexagonal type I crystals were present in the sample GLAS24  
20 of the *red cow* 1D103, in GLAS9 corresponding to the *signs* 1G223, in GLAS11  
21 corresponding to the *red deer* 1G212 (size range of 100 to 250 nm) as well as in GLAS63  
22 (Fig 8a) corresponding to the *red cow's* horn 1G206. Type II haematite was found in  
23 GLAS26 for the *red calf* 1D108 (Fig. 8b).  
24  
25

26 For the most part, haematite crystals could be found in association with hydroxyapatite  
27 crystals in red, yellow and brown flat paints of the *Bull Rotunda* such as in the *red cow*  
28 (1G206) and in the *red cow* 1D108 (GLAS26, Fig. 8c). By contrast, red lines or dots such  
29 as the red spot GLAS119, the *signs* 1G223 (GLAS9) and the red lines underlining the  
30 black horns of the *big bull* 1G203 (GLAS 8) as well as the desquamated sample LAS121  
31 did not contain any hydroxyapatite. There were also a few black samples (the black outline  
32 of the *black and yellow deer* 1G214 (GLAS12), the black dots 1D114 (GLAS21) and the  
33 *cave bear's* ear (GLAS25), that contained hydroxyapatite, but its presence seems to be  
34 linked to yellow, brown or red paints underlaid or located very close to the black samples.  
35  
36

37 TEM-EDS also showed the local presence of a titanium (Ti) oxide phase associated with  
38 haematite crystals in the sample GLAS26 of the *red cow* 1D108 and the sample GLAS11  
39 of the *red deer* 1G212. The type of Ti oxide phase could not be determined because it  
40 was not crystalline enough.  
41  
42

43 The yellow samples were not studied extensively using TEM but some electron diffraction  
44 patterns confirmed the presence of the Fe oxyhydroxide (goethite  $\text{FeOOH}$ ) structure in  
45 good agreement with the yellow colour.  
46

47 Brown paints contain haematite and cryptomelane in the form of lamellar sheets and  
48 longitudinal crystals, respectively. The presence of one Fe oxide and one Mn oxide phase  
49 was consistent with SEM-EDS analyses. The presence of hydroxyapatite nanocrystals  
50 was also observed in brown paints by TEM.  
51  
52  
53  
54  
55  
56  
57  
58  
59  
60

## Discussion. New information in the ornamentation steps of the *Bull Rotunda*

### Chemical-mineralogical grouping of figures corresponding to one execution step at the *Bull Rotunda*

The TEM-EDS-SAED results were grouped according to the postulated creation steps in order to check their consistency in terms of chemical and crystallographic phases present in the corresponding paint pot:

#### 1. Step of *monochromatic horses*

Only one sample was studied of step 1 (GLAS16) by SEM, as the homogeneity of the figures this step was not questioned. Its black corresponded to a Ba-bearing Mn oxide in the form of rolled needles. The additional presence of aluminosilicates was detected.

#### 2. Step of *bichrome and polychrome horses* including the *unicorn*

Nine samples of this creation step were studied corresponding to black, red and brown colours. All black matter corresponds to a Ba-bearing Mn oxide either in the form of sheets, needles, spherical grains or plates according to SEM. TEM showed the presence of cryptomelane. A very unique figure in the *Bull Rotunda* is the black *unicorn* corresponding with the samples GLAS1 and GLAS2. A Ba-bearing Mn oxide was identified in the two samples with a very similar morphology corresponding both to the horn and the beard of the *unicorn*, but the paint matter was applied in two different application modes. One implies a brush and the other spraying or blowing. This difference in application mode could support the separation of the horns from the rest of the body of the *unicorn*. However, the close association of the horns and the body of the *unicorn* is underlined by the fact that the end of the line of the horns continues more than 15 cm along with the lines of the head (Aujoulat, 2004). The same type of paint matter found in the horn and the beard of the *unicorn* reinforces this coherence and association of these elements in one figure despite different modes of application.

A red flat paint sample (GLAS 5) coming from the *big horse* 1G202 were also studied. The sample showed iron oxide in the form of haematite that was associated with an aluminosilicate and small amounts of a Ca-P phase, likely hydroxyapatite. We indicated the red colour in the *horse* 1G202 in this execution step with 2\* in Table 1 because it cannot be ascertained by chemical and mineralogical characterization that this colour was added during this execution step.

Brown colour was studied in the *brown horse* 1G204 (GLAS10, 61 and 62). Its paint matter was dominated by the presence of aluminosilicates rich in Fe and Mn. The Ca-P-based phase (hydroxyapatite) was also identified in the brown paint. The shape of the hydroxyapatite nanocrystals in the sample GLAS 62 indicated that they could have originated from reindeer antler in this particular case (Chadefaux et al., 2008).

It is possible that the Ca-P-based phase, hydroxyapatite, was deliberately added in order to change the consistence of the paint matter. It can also originate from the use of antler tools in the paint preparation. Taphonomy might also be an explanation for the formation of hydroxyapatite on cave walls in karst environments (Chalmin et al., 2017; Chalmin and Reiche, 2013). Finally, hydroxyapatite can be naturally associated to haematite from natural origin (Cornell and Schwertmann, 2003).

1  
2  
3 If hydroxyapatite originated from a natural mixture with haematite, it would likely have been  
4 found in all samples, which was not observed here. It was found systematically in the red  
5 and brown flat paints but was absent in the red drawing lines. Therefore, its presence  
6 seems to be related to red and brown paints applied in thin layers. Indeed, haematite  
7 nanocrystals might be intentionally diluted in other media because of its strong colouring  
8 properties giving rise to lighter red and brown colours. The systematic presence of  
9 hydroxyapatite in the red and brown flat paints indicates likely a similar geological origin  
10 of the paint matter and strengthens the hypothesis of the homogeneity of the paint  
11 preparation of this step and hence the synchronicity of the creation of these figures.  
12  
13

### 14 3. Step of the *black bulls*

15  
16 Ten samples corresponding to figures executed in the step 3 were examined.

17  
18 The black paint matter generally corresponded to Ba-bearing Mn oxides with various  
19 morphologies including longitudinal single crystals, rolls of needles, rods, “desert roses”,  
20 sheets and spherical grains. Their crystallographic phases corresponded to cryptomelane  
21 and/or hollandite. The chemical and crystallographic composition of this *black bulls* was  
22 very consistent. It was also characterized by the absence of a Ca-P phase. The *black sign*  
23 1G226 in *big bull* 1G205 as well as the *black punctuations* 1D114 in the body of the *black*  
24 *bull* 1D102 showed an analogous composition to that of the corresponding *black bulls* of  
25 this step and were thus confirmed to belong to the same ornamentation step.  
26

27  
28 However, the *cross-shaped sign* 1D112 was revealed to be different in composition with  
29 respect to the two *black bulls* 1D101 and 1D102 represented beside it. Magnetite was  
30 detected along with cryptomelane in this black sign (GLAS 19). The cross-shaped sign  
31 1D112, should thus be attributed to another creation step and is consequently indicated  
32 as such (3) in Table 1.  
33

34 Todorokite, another crystallographic Mn oxide phase, was found with cryptomelane and  
35 hollandite in one sample of the abdomen line of the *black bull* 1D101 (GLAS 23). Its  
36 presence in GLAS 23 is probably linked to a repaint on the ventral bull strip evidenced by  
37 macrophotography.  
38

39 Besides black paints, haematite was found in the red lines on the horns of the *black bull*  
40 1G203 and dots (GLAS 8). They were either hexagonal single crystals type I or sheets.  
41 They also contained aluminosilicates rich in K and Ti. As the third step was consistently  
42 executed with black paint matter, it is questionable if the red lines of the horns belong to  
43 this step. Therefore, the samples of the red horns were indicated as 3\* in Table 1. They  
44 might be related to the creation step 5 as described below. The paint matter found in the  
45 signs 1G223 (GLAS 9) on the left-hand side of the *Bull Rotunda* in front of the bull 1G203  
46 cannot be directly related to the haematite type found in the red lines of the bull 1G203  
47 and might belong to another execution step. They were also indicated as step 5 in Table  
48 1.  
49  
50

### 51 4. Step of the *red cows* and red dots on *black bull*

52  
53 Nine red samples were studied from the figures of step 4. The red colour was related to  
54 the presence of haematite in different shapes as observed by TEM. Lamellar sheets with  
55 hexagonal single crystals type I and trapezoidal single crystals type II were found with  
56  
57  
58  
59  
60

1  
2  
3 polycrystalline clusters (hyper-dispersed nanocrystals). These morphologies were  
4 common habits for haematite of sedimentary origin (Cornell and Schwertmann, 2003).  
5 Haematite was associated with quartz, Na- and K-rich aluminosilicates, calcium carbonate  
6 and in a quasi-systematic manner to a Ca-P-based (hydroxyapatite) phase. In the sample  
7 GLAS 26 corresponding to the red calf 1D108, hydroxyapatite with the characteristic  
8 features of that of reindeer antler (Chadefaux et al., 2008) was identified along with  
9 haematite type II. The chemical and mineralogical composition of this creation step is very  
10 consistent. Interestingly, the same association of Fe oxide-based (haematite) colouring  
11 matter with the presence of a Ca-P-phase (hydroxyapatite) was observed as for the  
12 second step of *bi- and polychrome horses*. This strengthened the observation of the  
13 systematic presence of hydroxyapatite in red and brown flat paints.  
14  
15

16 The red desquamated sample LAS121 found on the soil showed a very similar  
17 mineralogical composition, which is consistent with that of *red cows* 1D108 et 1D103.  
18 Therefore, this sample can be associated to the creation step 4.  
19

20 The sample GLAS119 from the bench contained polycrystalline haematite and haematite  
21 in sheets as well as an important amount of Al-rich clay, but no calcite. The bench  
22 composition was thus different from that of the wall.  
23

#### 24 5. Step of *bichrome deer* 25

26 Three samples of the creation step 5 were investigated (GLAS11-13). They showed a Ba-  
27 based Mn oxide and haematite or goethite. The Ba-bearing Mn oxide showed fibrous  
28 plates or filaments, whereas haematite single crystals corresponded to type I. The  
29 haematite phase was rich in Ti. The presence of Ti in haematite crystals indicated ilmenite  
30 or another Ti-Fe based mineral  $Fe_xTi_yO_z$ , which could be helpful to identify the raw  
31 material source as some magmatic rock. Some aluminosilicates, calcium carbonate and  
32 systematically a Ca-P-phase (hydroxyapatite) were found in the paint matter. The  
33 presence of aluminosilicates and calcium carbonate could be linked to the cretaceous  
34 limestone substrate. This step seemed also consistent with regard to its chemical and  
35 mineralogical composition of the figures. As mentioned above, the mineralogical features  
36 of the red horns of the *black bull* 1G203 (GLAS8, step 3\*) corresponding to hexagonal  
37 single crystals type I or sheets were similar to the samples from the *bichrome deer* (GLAS  
38 11) and can thus be related to this execution step.  
39  
40

#### 41 Other step: isolated *cave bear* 42

43 The *cave bear* figure sampled in GLAS25 and GLAS117 was hidden in the path of the  
44 ventral strip of the bull 1D101. The idea of a separate, probably later, creation is supported  
45 by the different chemical and mineralogical composition of the cave bear paint matter with  
46 respect to the large *black bull* 1D101 (GLAS 22 and 118, step 3). This *bull* was executed  
47 with a mixture of two different types of black Ba-bearing Mn oxides (cryptomelane and/or  
48 hollandite) whereas the *cave bear* contained a different mixture of a pure Mn oxide and  
49 hydroxide (pyrolusite and manganite) in the form of needles in mikado-shape and Ba-  
50 bearing Mn oxide (romanechite). The particular composition of the *cave bear* excluded its  
51 correspondence to any of the five creation steps of the *Bull Rotunda*.  
52  
53  
54  
55  
56  
57  
58  
59  
60



1  
2  
3 Figure 9 summarizes the different creation steps in terms of the chemical and  
4 mineralogical composition of the paint pots observed in different representations of the  
5 *Bull Rotunda* of the Lascaux cave.  
6  
7

8  
9 b) Interpretation of the execution sequence of the *Bull Rotunda* in terms of temporality of  
10 the living  
11

12 The cave of Lascaux was probably much frequented, but was not a settlement site. The  
13 subsistence hunter-gatherers had camps likely at different locations with respect to their  
14 settlement sites. At the camps, they crossed and hunted the animal herds at different  
15 seasons. The construction of the *Bull Rotunda* ornamentation in several creation steps of  
16 monothematic animal depictions could be related to the natural rhythm of transhumance  
17 in the cold Palaeolithic landscape, e.g. seasons (Aujoulat, 2004; Geneste, 2021).  
18

19 Each creation step translates the perception of the temporality of the living and likely  
20 represents each season. The *horses* (steps 1 and 2) represent the end of winter and the  
21 start of spring. The series of *black bulls* (step 3) and *red cows* (step 4) corresponds to  
22 summer, and the *deer* represents autumn (step 5). Lastly, the *cave bear* might represent  
23 winter as hibernating animal in these caves. The insulated figure, namely the *unicorn*, is  
24 difficult to interpret in terms of living temporality, although the *unicorn* could be associated  
25 with the *horse* series (steps 1 and 2).  
26  
27

28 c) Comparison with previous results obtained on insulated scenes of other rooms in the  
29 Lascaux cave and with other cave sites at a regional scale  
30

31 The electron microscopy study of the black paint matter used for the *Bull Rotunda*  
32 confirmed the presence of Ba-bearing Mn oxides in the form of hollandite, cryptomelane  
33 (with Ba and K) or todorokite. These pigments were already identified in other  
34 representations of the Lascaux cave (e.g. *scène du Puits*, *blasons*, *bisons adossés*),  
35 where additionally pyrolusite (pure Mn oxide), romanechite (with Ba), manganite and  
36 magnetite were found in single representations. The presence of pyrolusite and manganite  
37 was confirmed in the isolated figure of the *cave bear* of the *Bull Rotunda*. Its composition  
38 (a mixture of pyrolusite, manganite and romanechite) was similar to that of the falling horse  
39 and to the dark pigment blocks of *Diverticule axial* of the Lascaux cave. Pyrolusite and  
40 romanechite were the main components of some dark blocks found during excavations in  
41 particular in *crayons* no. 53 and 6 (Chalmin et al., 2004). This might indicate that the cave  
42 bear was executed at another moment, possibly at the same time when the falling horse  
43 of the *Diverticule Axial* was created. It should be noted that there were two other engraved,  
44 but not painted *cave bear* representations in the *Passage* of the Lascaux cave (Man-  
45 Estier, 2009).  
46  
47  
48

49 Furthermore, there is a parallel between presence of todorokite identified in GLAS23 of  
50 the ventral stripe of *black bull* 1D101 and another figure (*blasons*) within the ornamentation  
51 of the *Nef* of the Lascaux cave and the colouring blocs found on the soil (Chalmin et al.,  
52 2006). Pyrolusite and todorokite were found in the rectangle 43 of the *blasons*.  
53 Romanechite was mixed with todorokite in the rectangle 47. Cryptomelane and todorokite  
54 were found in the rectangles 49 and 52. Therefore, todorokite, a special crystallographic  
55 phase identified in the repainted ventral stripe of the *black bull* is not unknown in other  
56  
57  
58  
59  
60



rooms of the Lascaux cave, a fact that suggests a possible creation of this overpaint at another moment as the execution step of the *blasons*.

The black *cross-shaped sign* 1D112 was also revealed to be different in its composition to the two nearby *black bulls* 1D101 and 1D102. The presence of magnetite in the *sign* 1D112, its particular paint matter of two mixed Fe and Mn oxide-based black mineral phases, corresponds to that found in the right *bison* (GLAS103 and 105) of the *bisons adossés* in the *Nef* of the Lascaux cave (Vignaud et al., 2006). This, too, might also have been a later addition to the panel.

Concerning the red paints, different morphologies of haematite were already observed in the red paints of the *blasons* and *bisons adossés*. Strikingly, the presence of the Ca-P phase is observed in a quasi-systematic way in the Fe oxide-based paints of the *Bull Rotunda* but Ca-P was absent in the desquamated red sample LAS121 collected on the soil. Its presence in addition to the paint matter seems to be a characteristic marker of the paint preparation involved in the execution steps of the *Bull Rotunda*.

At a regional scale, the black Mn-based paint matter identified by non-invasive methods such as portable X-ray fluorescence and micro-Raman analyses in other Upper Palaeolithic decorated cave sites such as that of Rouffignac and Font-de-Gaume in Dordogne showed a different mineralogical composition with respect to those found in this study in Lascaux. According to our current knowledge, the black matters of Rouffignac and Font-de-Gaume are mixtures of romanechite and pyrolusite (Gay et al., 2020; Trosseau et al., 2021), whereas that of Lascaux showed mainly K-rich and cryptomelane-based Mn oxide. The collected paint matter of each site likely came from different sources and should not be considered on a more regional scale (in the range of some ten to hundred km) because there was a lot of choice in the region.

## Conclusions

Scanning and transmission electron microscopy of 32 micro-samples of the figures of the Bull Rotunda of the Lascaux cave allowed the extensive study of the black and red paint matters with their associated mineralogical phases at micro- and nanoscale. While the red paint matter only contained one pigment, haematite, and the differentiation can be performed by the associated crystallographic phases, black paint matters could be distinguished thanks to the presence of different crystallographic Mn oxide phases such as cryptomelane and hollandite. These phases were shown to be Ba- and/or K-bearing Mn oxides. On this basis it was possible to confirm the five consistent creation steps of the ornamentation of the *Bull Rotunda* in the Lascaux cave proposed by previous stylistic and superimposition studies. Our new results also allowed corroborating the hypothesis to read the figures in terms of the natural life cycle of the Upper Palaeolithic hunter-gatherer society, e.g. seasons.

Some particular representations such as the black *cave bear* and one of the *cross-shaped signs* were highlighted, and understood to likely have been added at posterior moments and by other “artists” operating in deeper rooms as the *Nef* and the *Diverticule axial* of this

1  
2  
3 extraordinary cave. This was shown by the parallels in terms of paint pot composition with  
4 figures from deeper galleries in the Lascaux cave.  
5

6 A comparison of the black paint matter of the *Bull Rotunda* (mainly cryptomelane, except  
7 for the *cave bear*) with that of other Palaeolithic cave sites in the Dordogne such as  
8 Rouffignac and Font-de-Gaume (generally pyrolusite and romanechite) revealed the use  
9 of different pigments in these caves indicating distinct colouring matter provenience.  
10

### 11 **Acknowledgments**

12  
13 We gratefully acknowledge the support and discussions with H el ene Salomon during  
14 sampling on site and after. She is also thanked for having provided the SEM micrographs.  
15 Fran oise Pillier is thanked for her support during TEM observations and sample  
16 preparation. Anne Maigret, photographer at the C2RMF, is kindly thanked for scanning  
17 the transmission electron micrograph negatives. Nicolette is kindly acknowledged for the  
18 revision of the English language. The DRAC Nouvelle Aquitaine is acknowledged for the  
19 support of this study. Norbert Aujoulat who passed away is especially acknowledged for  
20 his fundamental work and understanding of Lascaux cave art. We dedicate this publication  
21 to his memory.  
22  
23

### 24 **References**

25 Aujoulat, N., 2004. Lascaux: le geste, l'espace et le temps, Arts rupestres. Seuil, Paris.  
26

27 Aujoulat, N., Chalmin, E., Vignaud, C., Menu, M., 2002. Lascaux : les pigments noirs de  
28 la Sc ene du puits. 10es journ ees de la Section fran aise de l'institut international de  
29 conservation (SFIC) L'art avant l'histoire. Conservation de l'Art Pr ehistorique, Paris, 23-  
30 24 mai 2002, p. 5-14.  
31

32 Chadeaux, C., Vignaud, C., Menu, M., Reiche, I., 2008. Multianalytical Study of  
33 Palaeolithic reindeer antler. Discovery of Antler traces in Lascaux pigments by TEM.  
34 Archaeometry 50, 516–534. <https://doi.org/10.1111/j.1475-4754.2008.00373.x>  
35

36 Chalmin, E., 2003. Caract erisation des oxydes de mangan ese et usage des pigments  
37 noirs au Pal eolithique sup erieur (PhD Thesis). Universit e de Marne la Vall e.  
38

39 Chalmin, E., H erl e, S., Reiche, I., 2017. Taphonomy on the Surface of the Rock Wall:  
40 Rock-Paint-Atmosphere Interactions, in: David, B., McNiven, I.J. (Eds.), The Oxford  
41 Handbook of the Archaeology and Anthropology of Rock Art. Oxford University Press.  
42 <https://doi.org/10.1093/oxfordhb/9780190607357.013.47>  
43

44 Chalmin, E., Menu, M., Pomi es, M.-P., Vignaud, C., Aujoulat, N., Geneste, J.-M., 2004.  
45 Les blasons de Lascaux. L'Anthropologie 108, 571–592.  
46 <https://doi.org/10.1016/j.anthro.2004.12.001>  
47

48 Chalmin, E., Reiche, I., 2013. Synchrotron X-Ray Microanalysis and Imaging of  
49 Synthetic Biological Calcium Carbonate in Comparison With Archaeological Samples  
50 Originating from the Large Cave of Arcy-sur-Cure (28000-24500 BP, Yonne, France).  
51 Microsc. Microanal. 19, 1523–1534. <https://doi.org/10.1017/S1431927613013342>  
52

53 Chalmin, E., Vignaud, C., Salomon, H., Farges, F., Susini, J., Menu, M., 2006. Minerals  
54 discovered in paleolithic black pigments by transmission electron microscopy and micro-  
55  
56  
57  
58  
59  
60

1  
2  
3 X-ray absorption near-edge structure. Appl. Phys. A 83, 213–218.  
4 <https://doi.org/10.1007/s00339-006-3510-7>  
5

6 Cornell, R.M., Schwertmann, U., 2003. The Iron Oxides: Structure, Properties,  
7 Reactions, Occurrences and Uses, 1st ed. Wiley. <https://doi.org/10.1002/3527602097>  
8

9 Ducasse, S., Langlais, M., 2019. Twenty years on, a new date with Lascaux.  
10 Reassessing the chronology of the cave's Paleolithic occupations through new 14C AMS  
11 dating. Paléo 130–147. <https://doi.org/10.4000/paleo.4558>  
12

13 Fritz, C., Tosello, G., 2015. From Gesture to Myth: Artists' techniques on the walls of  
14 Chauvet Cave. Palethnologie. <https://doi.org/10.4000/palethnologie.876>  
15

16 Gay, M., Plassard, F., Müller, K., Reiche, I., 2020. Relative chronology of Palaeolithic  
17 drawings of the Great Ceiling, Rouffignac cave, by chemical, stylistic and  
18 superimposition studies. J. Archaeol. Sci. Rep. 29, 102006.  
19 <https://doi.org/10.1016/j.jasrep.2019.102006>  
20

21 Geneste, J.-M., 2021. Les grandes lignes d'un monde mythique insoupçonné. Des  
22 rythmes, de la temporalité et de la place du sujet dans l'art rupestre paléolithique. Afr.  
23 Stud. 9–27.  
24

25 Laming-Empeire, A., 1959. Lascaux : Paintings and Engravings, Harmondsworth. ed.  
26 Pelican Books, Middlesex, Engl. ; Baltimore, Maryland.  
27

28 Leroi-Gourhan, A., Allain, J. (Eds.), 1979. Lascaux inconnu, Supplément à "Gallia  
29 préhistoire." Editions de Centre national de la recherche scientifique, Paris.  
30

31 Man-Estier, E., 2009. Les ursidés au naturel et au figuré pendant la préhistoire  
32 (Sciences de l'Homme et Société.). Muséum National d'Histoire Naturelle, Paris, France.  
33

34 Trosseau, A., Maigret, A., Coquinot, Y., Reiche, I., 2021. *In situ* XRF study of black  
35 colouring matter of the Palaeolithic figures in the Font-de-Gaume cave. J. Anal. At.  
36 Spectrom. 36, 2449–2459. <https://doi.org/10.1039/D1JA00202C>  
37

38 Vignaud, C., Salomon, H., Chalmin, E., Geneste, J.-M., Menu, M., 2006. Le groupe  
39 des « bisons adossés » de Lascaux. Étude de la technique de l'artiste par analyse  
40 des pigments. L'Anthropologie, Art préhistorique 110, 482–499.  
41 <https://doi.org/10.1016/j.anthro.2006.07.008>  
42  
43  
44

#### 45 **Data availability statement**

46 The data are available through request to the corresponding author.  
47  
48  
49

#### 50 **Figure and table captions**

51  
52  
53 Figure 1. Lascaux cave map with location of the left and right wall of *Bull Rotonda*. ©  
54 *Bassier*  
55  
56  
57  
58  
59  
60

1  
2  
3 Figure 2. Left wall of *Bull Rotonda* with location of the microsamples (GLASXX).  
4 Numbering 1G10X corresponds to each entity: black monochrome figures are indicated in  
5 black, red monochrome figures are indicated in red and bichrome figures are indicated in  
6 green. © I. Reiche, CNRS, adapted from N. Aujoulat.  
7

8 Figure 3. Right wall of *Bull Rotonda* with location of the micro-samples (GLASXX). LAS121  
9 corresponds to a desquamated sample from the ground. Numbering 1D10X corresponds  
10 to each entity: black monochrome figures are indicated in black and red monochrome  
11 figures are indicated in red. © I. Reiche, CNRS, adapted from N. Aujoulat.  
12

13 Figure 4. Optical micrographs: (a and b) red desquamation LAS121 sample, (b) prepared  
14 as a cross section; (c and d) black samples: (c) *big bull* 1D101 GLAS22 and (d) *cave bear*  
15 GLAS 117. © C. Vignaud  
16

17 Figure 5. Scanning electron micrographs (SEM in BSE mode): (a and b) cross section las  
18 121 sample, (b) detail on punctual red pigment; (c and d) *cave bear* GLAS117, Mn oxide,  
19 Ba-bearing Mn oxide and Ca oxide, (d) detail on Ba-bearing Mn oxide. ©E. Chalmin and  
20 H. Salomon  
21  
22

23 Figure 6. Transmission electron micrographs of black phases detected in the black *big bull*  
24 1D101 samples GLAS 22 and 23. (a and b) GLAS 22 on the its back line, (c) GLAS 23 on  
25 its black ventral strip: (a) hollandite, monoclinic, zone axis [0-11], (b) cryptomelane,  
26 monoclinic, zone axis [001], (c) todorokite, monoclinic, characteristic meshwork crystals.  
27 © E. Chalmin and C. Vignaud  
28

29 Figure 7. Transmission electron micrographs with corresponding electron diffraction  
30 patterns of the black phases detected in the *cave bear* sample GLAS 117 (a, b and c) and  
31 in the *cross* 1D112 sample GLAS19 (d): (a) manganite, monoclinic, zone axis [2-10], (b)  
32 romanechite, monoclinic, zone axis [021], (c) pyrolusite, tetragonal, zone axis [12-1], (d)  
33 magnetite Fe<sub>3</sub>O<sub>4</sub>, face-centered cubic, zone axis [10-1]. © E. Chalmin and C. Vignaud  
34  
35

36 Figure 8. Transmission electron micrographs with corresponding electron diffraction  
37 patterns of the red phases detected in the *red cow* 1G206 and the *red calf* 1D108: a)  
38 haematite crystal of hexagonal shape in GLAS 63 corresponding to the *red cow* (1G206)  
39 and corresponding electron diffraction (trigonal), b) Haematite crystal of trapezoidal shape  
40 found in micro-samples GLAS 26 corresponding to the *red calf* 1D108, c) Haematite  
41 nanocrystals mixed within hydroxyapatite in GLAS 26 and corresponding TEM-EDX  
42 spectrum indicating the presence of a Ca-P-based phase (hydroxyapatite) and Fe oxide  
43 trapped in an aluminosilicate matrix. © C. Vignaud  
44  
45

46 Figure 9. Schematic overview of the different creation steps in terms of the chemical and  
47 mineralogical composition of the paint pots observed in different representations of the  
48 *Bull Rotonda* of the Lascaux cave. © Conception: I. Reiche, C. Vignaud and E. Chalmin;  
49 Realization: E. Chalmin  
50

51 Table 1. Summary of the morphological, mineralogical and chemical features at the micro-  
52 and at nanoscale of the studied micro-samples of the *Bull Rotonda*. If the creation step is  
53 shown in brackets it means that its attribution to this step has changed according to the  
54 determined mineralogical composition. If an asterisk is indicated at the number of the  
55 execution step it means that this attribution is questionable and cannot be ascertained.  
56  
57  
58  
59  
60

1  
2  
3  
4  
5  
6  
7  
8  
9  
10  
11  
12  
13  
14  
15  
16  
17  
18  
19  
20  
21  
22  
23  
24  
25  
26  
27  
28  
29  
30  
31  
32  
33  
34  
35  
36  
37  
38  
39  
40  
41  
42  
43  
44  
45  
46  
47  
48  
49  
50  
51  
52  
53  
54  
55  
56  
57  
58  
59  
60

For Peer Review

1  
2  
3  
4  
5  
6  
7  
8  
9  
10  
11  
12  
13  
14  
15  
16  
17  
18  
19  
20  
21  
22  
23  
24  
25  
26  
27  
28  
29  
30  
31  
32  
33  
34  
35  
36  
37  
38  
39  
40  
41  
42  
43  
44  
45  
46  
47  
48  
49  
50  
51  
52  
53  
54  
55  
56  
57  
58  
59  
60



Figure 1. Lascaux cave map with location of the left and right wall of Bull Rotonda. © Bassier

137x97mm (118 x 118 DPI)



1  
2  
3  
4  
5  
6  
7  
8  
9  
10  
11  
12  
13  
14  
15  
16  
17  
18  
19  
20  
21  
22  
23  
24  
25  
26  
27  
28  
29  
30  
31  
32  
33  
34  
35  
36  
37  
38  
39  
40  
41  
42  
43  
44  
45  
46  
47  
48  
49  
50  
51  
52  
53  
54  
55  
56  
57  
58  
59  
60

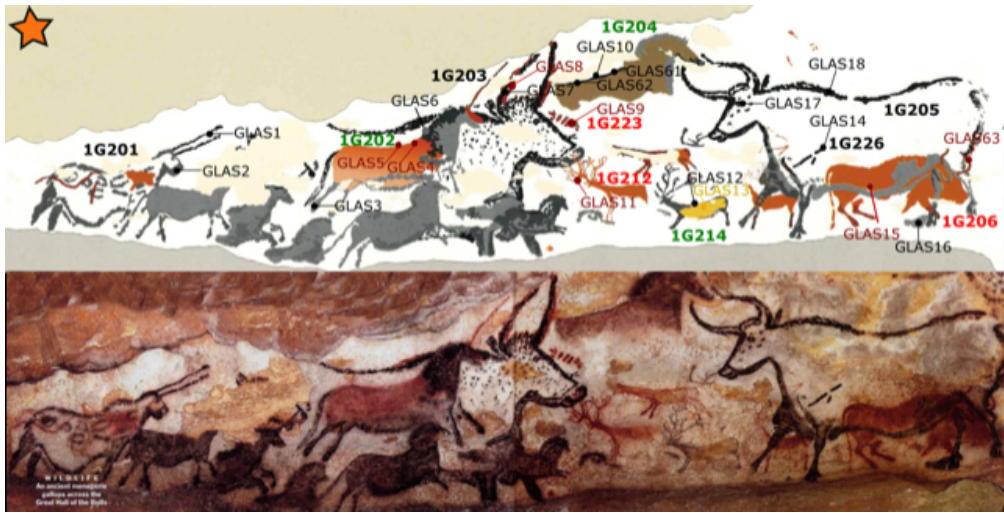


Figure 2. Left wall of Bull Rotonda with location of the microsamples (GLASXX). Numbering 1G10X corresponds to each entity: black monochrome figures are indicated in black, red monochrome figures are indicated in red and bichrome figures are indicated in green. © I. Reiche, CNRS, adapted from N. Aujoulat.

275x139mm (59 x 59 DPI)

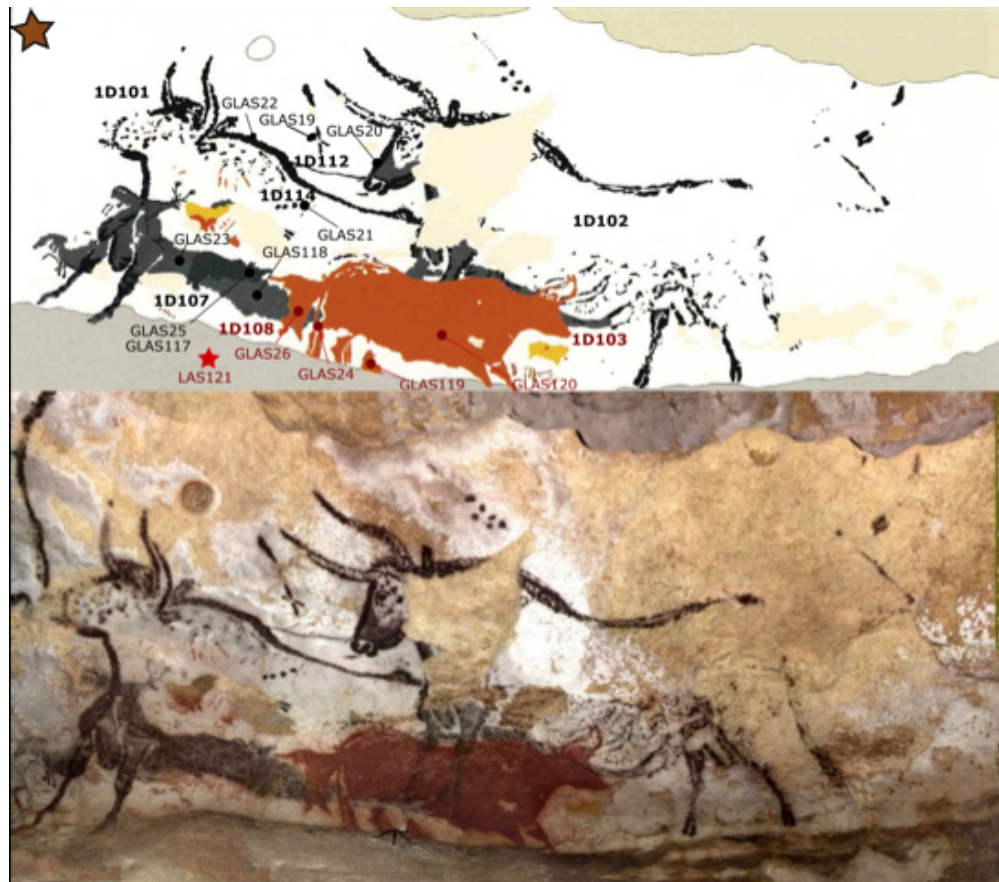


Figure 3. Right wall of Bull Rotonda with location of the micro-samples (GLASXX). LAS121 corresponds to a desquamated sample from the ground. Numbering 1D10X corresponds to each entity: black monochrome figures are indicated in black and red monochrome figures are indicated in red. © I. Reiche, CNRS, adapted from N. Aujoulat.

117x103mm (118 x 118 DPI)

1  
2  
3  
4  
5  
6  
7  
8  
9  
10  
11  
12  
13  
14  
15  
16  
17  
18  
19  
20  
21  
22  
23  
24  
25  
26  
27  
28  
29  
30  
31  
32  
33  
34  
35  
36  
37  
38  
39  
40  
41  
42  
43  
44  
45  
46  
47  
48  
49  
50  
51  
52  
53  
54  
55  
56  
57  
58  
59  
60

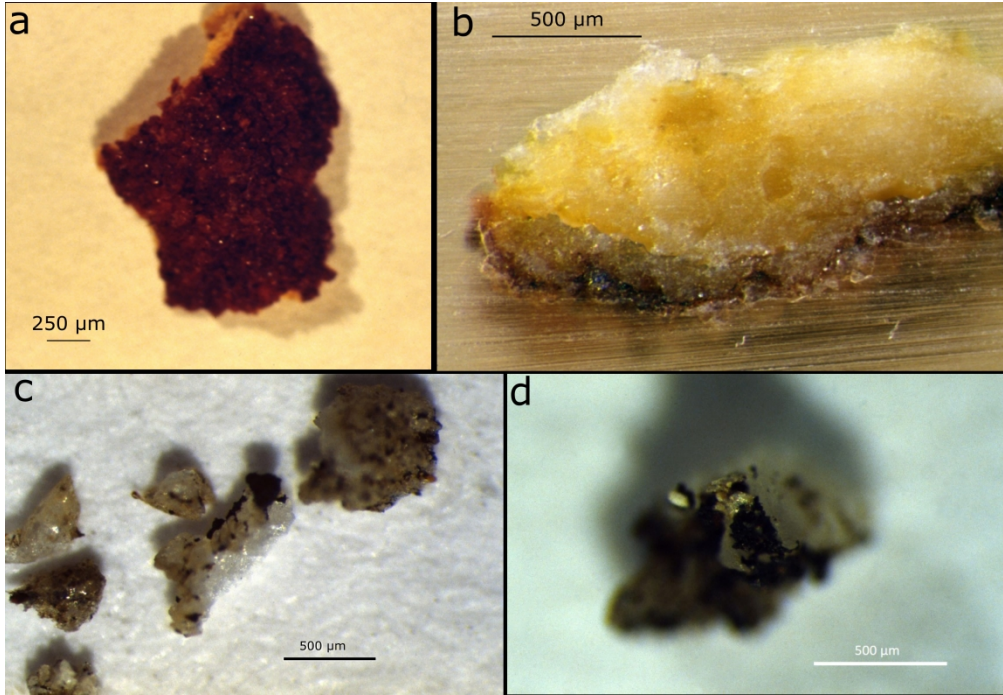


Figure 4. Optical micrographs: (a and b) red desquamation LAS121 sample, (b) prepared as a cross section; (c and d) black samples: (c) big bull 1D101 GLAS22 and (d) cave bear GLAS 117. © C. Vignaud

748x517mm (118 x 118 DPI)

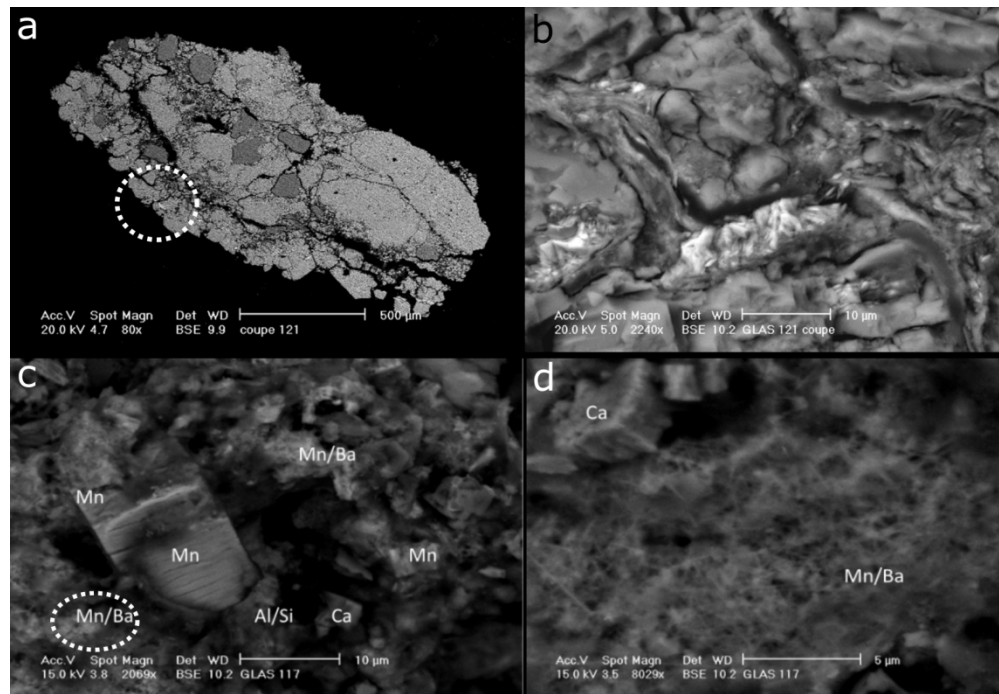


Figure 5. Scanning electron micrographs (SEM in BSE mode): (a and b) cross section las 121 sample, (b) detail on punctual red pigment; (c and d) cave bear GLAS117, Mn oxide, Ba-bearing Mn oxide and Ca oxide, (d) detail on Ba-bearing Mn oxide. ©E. Chalmin and H. Salomon

758x521mm (59 x 59 DPI)

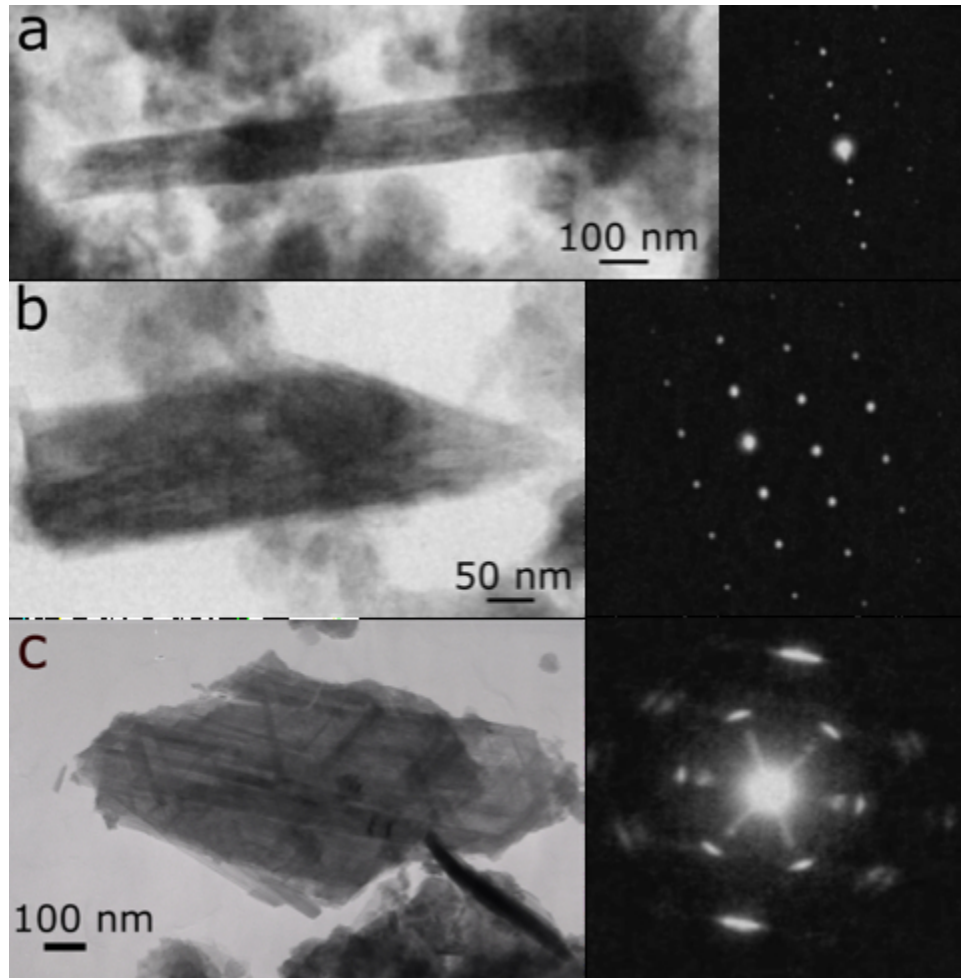


Figure 6. Transmission electron micrographs of black phases detected in the black big bull 1D101 samples GLAS 22 and 23. (a and b) GLAS 22 on the its back line, (c) GLAS 23 on its black ventral strip: (a) hollandite, monoclinic, zone axis  $[0-11]$ , (b) cryptomelane, monoclinic, zone axis  $[001]$ , (c) todorokite, monoclinic, characteristic meshwork crystals. © E. Chalmin and C. Vignaud

206x209mm (59 x 59 DPI)



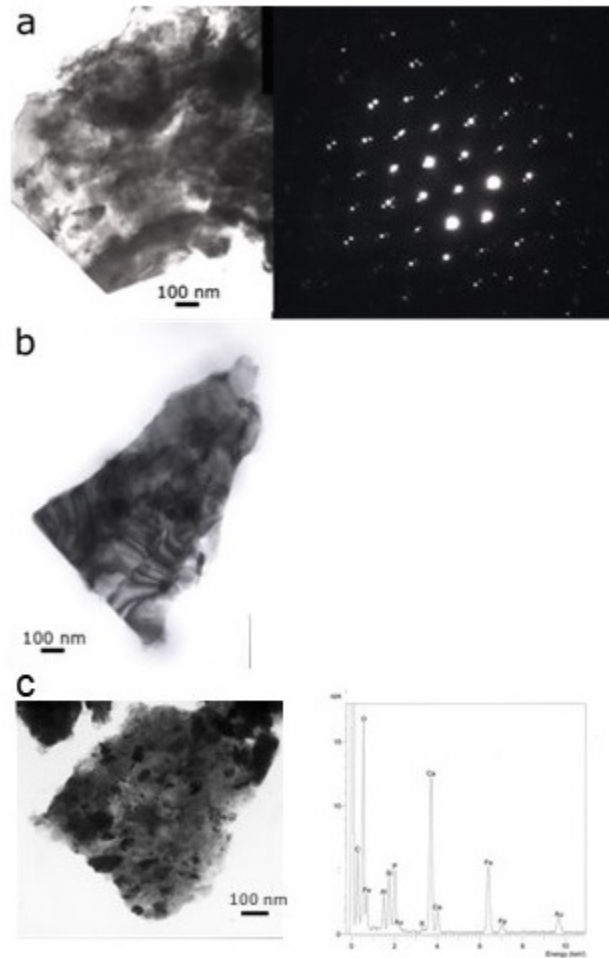


Figure 8. Transmission electron micrographs with corresponding electron diffraction patterns of the red phases detected in the red cow 1G206 and the red calf 1D108: a) haematite crystal of hexagonal shape in GLAS 63 corresponding to the red cow (1G206) and corresponding electron diffraction (trigonal), b) Haematite crystal of trapezoidal shape found in micro-samples GLAS 26 corresponding to the red calf 1D108, c) Haematite nanocrystals mixed within hydroxyapatite in GLAS 26 and corresponding TEM-EDX spectrum indicating the presence of a Ca-P-based phase (hydroxyapatite) and Fe oxide trapped in an aluminosilicate matrix. © C. Vignaud

84x128mm (96 x 96 DPI)



1  
2  
3  
4  
5  
6  
7  
8  
9  
10  
11  
12  
13  
14  
15  
16  
17  
18  
19  
20  
21  
22  
23  
24  
25  
26  
27  
28  
29  
30  
31  
32  
33  
34  
35  
36  
37  
38  
39  
40  
41  
42  
43  
44  
45  
46  
47  
48  
49  
50  
51  
52  
53  
54  
55  
56  
57  
58  
59  
60

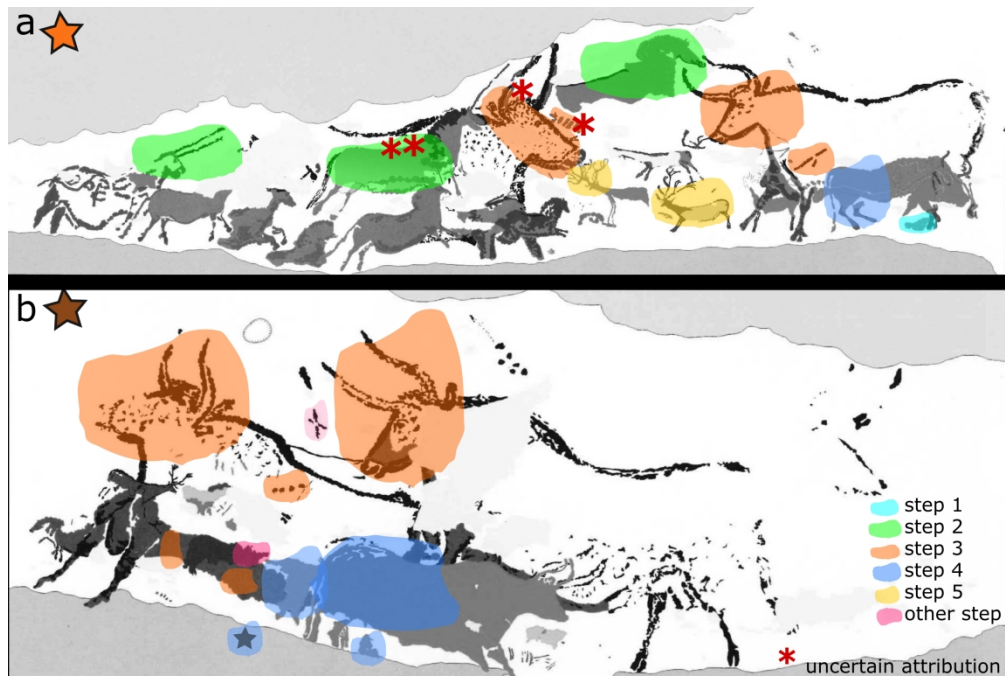


Figure 9. Schematic overview of the different creation steps in terms of the chemical and mineralogical composition of the paint pots observed in different representations of the Bull Rotunda of the Lascaux cave.  
© Conception: I. Reiche, C. Vignaud and E. Chalmin; Realization: E. Chalmin

756x505mm (118 x 118 DPI)

**Table 1.** Summary of the morphological, mineralogical and chemical features at the micro- and at nanoscale of the studied micro-samples of the Bull Rotunda. If the creation step is shown in brackets it means that its attribution to this step has changed according to the determined mineralogical composition. If an asterisk is indicated at the number of the execution step it means that this attribution is questionable and cannot be ascertained.

Hypothesized creation step	Figure	Sample number	Main colour / rendering	Other phases or elements	Inferred creation step
Results indicated	Type of paint matter		Crystal morphology	Additional minerals	
<b>1</b>	<b>Small black horse</b>	<b>GLAS16</b>	<b>Black / filling</b>		
	Mixed Mn oxide with Ba		Needle rolls	Aluminosilicates	<b>1</b>
<b>2</b>	<b>Unicorn 1G201</b>	<b>GLAS1</b>	<b>Black horn / continuous outline</b>		
	Mixed Mn oxide with Ba		Sheets 10µm x 1µm	Aluminosilicates	<b>2</b>
		<b>GLAS2</b>	<b>Black beard / tight punctuations</b>		
	Mixed Mn oxide with Ba and K		Sheets 10µm x 1µm	Aluminosilicates	<b>2</b>
<b>2</b>	<b>Big horse 1G202</b>	<b>GLAS3</b>	<b>Black back leg / continuous outline</b>		
	Mixed Mn oxide with Ba		Spherical grains of 0.5µm and sticks	Aluminosilicates Cl+Hg	
		<b>GLAS6</b>	<b>Black neckline / tight punctuations</b>		
	Mixed Mn oxide with Ba		Spherical grains of 0.5µm to 1µm	Silicate (absence of Al)	<b>2</b>
		<b>GLAS4</b>	<b>Red neckline / continuous outline</b>		<b>2*</b>
	Fe oxide		Sheets and plaquettes	Aluminosilicates and Mn traces	
		<b>GLAS5</b>	<b>Red flat colour / filling</b>		<b>2*</b>
	Fe oxide		Sheets and plaquettes	Ca/P phase, aluminosilicates and Mn traces	
<b>2</b>	<b>Brown horse 1G204</b>	<b>GLAS10</b>	<b>Brown / continuous outline</b>		

	Fe oxide + Mn oxide	Fe and Mn enriched aluminosilicates	Ca/P phase, Aluminosilicates, <b>calcium carbonate</b> , calcium sulfate	<b>2</b>
		<b>GLAS61</b>	<b>Proximal end of the black line of the back / continuous outline</b>	
	Mixed Mn oxide with Ba	Needles of 0.5 to 2.5µm length	Aluminosilicates, quartz, hair included in Mn oxide, Cl+Hg (pollution)	<b>2</b>
		<b>GLAS62</b>	<b>Brown distal end of back</b>	
	Fe oxide + Mn oxide	Sheets Fe/O, fibres Mn/O	Ca/P phase <b>Aluminosilicates</b>	
	Haematite, cryptomelane	Single crystals and sticks of 200 to 400 nm	Ca/P phase in the form of hydroxyapatite likely from reindeer antler	<b>2</b>
<b>3</b>	<b>Big bull 1G203</b>	<b>GLAS7</b>	<b>Black horn / continuous outline</b>	
	Mixed Mn oxide with Ba	Sheets inf. 1µm	Aluminosilicates	<b>3</b>
<b>3</b>		<b>GLAS8</b>	<b>Red horn / tight punctuations</b>	
	Fe oxide	Sheets 1-10µm	Aluminosilicates + K and Ti	<b>5</b>
<b>3</b>	<b>Signs 1G223</b>	<b>GLAS9</b>	<b>Red dots and lines / punctuations</b>	
	Fe oxide	Fibres	Aluminosilicates, <b>quartz</b> , K, Ti	
	Haematite	Hexagonal single crystals type I	-	<b>5</b>
<b>3</b>	<b>Black sign 1G226 in the body of 1G205</b>	<b>GLAS14</b>	<b>Black / punctuations</b>	
	Mixed Mn oxide with Ba and K	"Desert roses"	Ti	
	Cryptomelane and hollandite	Longitudinal single crystals	TiO <sub>2</sub>	<b>3</b>
<b>3</b>	<b>Big bull 1G205</b>	<b>GLAS17</b>	<b>Black eye / tight punctuations</b>	
	Mixed Mn oxide with Ba		Aluminosilicates grains 0.1µm piled up 0.5µm	<b>3</b>

		<b>GLAS18</b>	<b>Black back / continuous outline</b>	
	Mixed Mn oxide with Ba		Rolls of needles 2 x 0.1µm	Aluminosilicates + Al
	Cryptomelane and hollandite		Longitudinal single crystals	-
				<b>3</b>
<b>3</b>	<b>Cross 1D112 in front of the muzzle of 1D102</b>	<b>GLAS19</b>	<b>Black / continuous outline</b>	
	Mixed Mn oxide with Ba		Needles, rolls and sticks	aluminosilicates + quartz, Hg
	Cryptomelane and magnetite		Single crystals	-
				<b>(3) posterior to the decoration of the Bull Rotunda</b>
<b>3</b>	<b>Big bull 1D102</b>	<b>GLAS20</b>	<b>Black chamfer facing eye / punctuations</b>	
	Mixed Mn oxide with Ba		Spherical grains and sticks	aluminosilicates, quartz
	Cryptomelane		Longitudinal single crystals	-
				<b>3</b>
<b>3</b>	<b>Black punctuations 1D114 in the body of 1D101</b>	<b>GLAS21</b>		
	Mixed Mn oxide with Ba		Spherical grains and sticks	Ca/P phase, aluminosilicates and Hg (pollution)
	Cryptomelane		Longitudinal single crystals	-
				<b>3</b>
<b>3</b>	<b>Big bull 1D101</b>	<b>GLAS22</b>	<b>Black back / continuous outline</b>	
	Mixed Mn oxide with Ba		Rolls	aluminosilicates +Al, Hg
	Cryptomelane and hollandite			-
		<b>GLAS23</b>	<b>Black abdomen / punctuations</b>	outside the bear
<b>3</b>	Mixed Mn oxide with Ba		Rolls and sticks	aluminosilicates +Al, Hg
	Todorokite		Meshes	-
				<b>3*</b>
<b>3</b>		<b>GLAS118</b>	<b>Black abdomen / punctuations</b>	outside the bear
	Mixed Mn oxide with Ba		Sheets 1µm and needles	<b>Calcium carbonate</b>
	Cryptomelane		Rare small crystals	-
				<b>3*</b>

4	<b>Big red cow 1G206 GLAS15</b>	<b>Red flat colour / filling</b>		
	Fe oxide	Poor in oxide	<b>Ca/P phase</b>	<b>4</b>
		<b>GLAS63</b>	<b>Red left horn / filling</b>	
	Fe oxide	Needles and small plates	<b>Quartz</b>	
	Haematite	Hexagonal single crystals type I (and II), 1.2µm	-	<b>4</b>
4	<b>Red cow 1D103 GLAS24</b>	<b>Red tail / continuous outline</b>		
	Fe oxide	Spherical grains 0.1µm	Ca/P phase, aluminosilicates	
	Haematite	Lamellar sheets type I		<b>4</b>
		<b>GLAS120</b>	<b>Red / filling</b>	
	Fe oxide	<b>K-bearing alumina-silicates with Fe</b>	Calcite with pigment in the fissures	<b>4</b>
4	<b>Red calf 1D108 GLAS26</b>	<b>Red / filling</b>		
	Fe oxide		<b>Ca/P phase, Alumino-silicates + Fe, Ti, K</b>	<b>4</b>
	Haematite	Sheets type II and rods	Hydroxy-apatite likely from reindeer antler	<b>4</b>
4	<b>Red spot on bench seat GLAS119</b>	<b>Red spot under the red cow / punctuation</b>		
	Fe oxide		many Fe grains entrapped in K-bearing aluminosilicates and locally Na-bearing	
	Hematite	Hematite in sheets and polycrystalline hematite	-	<b>4</b>
4	<b>Wall desquamation: flake on the ground LAS121</b>	<b>Under the red cow</b>		
	Fe oxide	Porous calcite wall	aluminosilicates rich in Fe, K, Cl	
	Hematite	Hematite in sheets and polycrystalline of different crystal dimensions		<b>4</b>
5	<b>Two-headed deer 1G212 GLAS11</b>	<b>Red / continuous outline</b>		

	Fe oxide	Fibrous plates <1µm	Ca/P phase a few aluminosilicates, Ti	
	Hematite	Single crystals type I, 100-250nm	Ti	<b>5</b>
<b>5</b>	<b>Black and yellow deer 1G214 GLAS12</b>	<b>Black outline / continuous outline</b>		
	Mixed Mn oxide with Ba	Filaments 1µmx0.1µm	Ca/P phase	<b>5</b>
		<b>GLAS13</b>	<b>Yellow body / filling</b>	
	Fe oxide	Few material	Ca/P phase, <b>Ca carbonate</b> aluminosili-cates	<b>5</b>
<b>other</b>	<b>Bear 1D107</b>	<b>GLAS25</b>	<b>Black ear / punctuation</b>	
	Mn oxide and mixed Mn oxide with Ba	Grains and rods	Ca/P phase, aluminosili-cates, Mg	<b>posterior to the decoration of the Bull Rotunda</b>
	Pyrolusite, manganite and romanechite	Longitudinal single crystals		
		<b>GLAS117</b>	<b>Black muzzle / punctuation</b>	
	Mn oxide and mixed Mn oxide with Ba	Prisms of Mn oxide and needles Mn-Ba	big prisms of calcite and round quartz grains	<b>posterior to the decoration of the Bull Rotunda</b>
	Pyrolusite and romanechite	Needles in mikado-shape and longitudinal single crystals		

1  
2  
3  
4  
5  
6  
7  
8  
9  
10  
11  
12  
13  
14  
15  
16  
17  
18  
19  
20  
21  
22  
23  
24  
25  
26  
27  
28  
29  
30  
31  
32  
33  
34  
35  
36  
37  
38  
39  
40  
41  
42  
43  
44  
45  
46  
47  
48  
49  
50  
51  
52  
53  
54  
55  
56  
57  
58  
59  
60